Chapter 6
The Activity-Based Theoretical Na–K Geoindicators

Abstract Accepting that a single universally-working Na-K geothermometer does not exist and the Na-K geothermometers are controlled by the exchange reaction involving fully-ordered low-albite and variably-ordered adularia, from fully ordered maximum-microcline to completely disordered high-sanidine, the Na/K activity ratio of the aqueous solution is expected to be a function of both temperature and the ordering parameter of adularia, Z. However, the two limiting Na-K geothermometers involving low-albite and either high-sanidine (with $Z = 0$) or maximum-microcline (with $Z = 1$) give equilibrium temperatures differing by 125 ± 3 °C on average, in the range 100–350 °C, and have little usefulness. We used Multiple Regression Analysis to try to predict the ordering parameter of adularia based on the chemical characteristics of the 1013 selected reservoir liquids, but it turned out that Z is chiefly controlled by Na, K, and SiO_2. This is a disappointing result being affected by a circular argument. Therefore, for the moment, it is advisable to utilize the Na/K log activity ratio to estimate the ordering parameter Z of the hydrothermal adularia in hypothetical equilibrium with the considered aqueous solutions and to use this information in other geothermometers representing the subject of the following chapters.

We have already recalled that several previous authors (e.g., White 1965; Ellis 1970; Fournier 1979; Arnórsson et al. 1983; Giggenbach 1988; Michard 1990) suggested that the activities of Na^+ and K^+ ions in reservoir liquids are probably controlled by the exchange reaction (5.74) between hydrothermal alkali feldspars, which is rewritten here for convenience:

$$NaAlSi_3O_8 + K^+ = KAlSi_3O_8 + Na^+. \tag{6.1}$$

The possible involvement in reaction (6.1) of solid phases other than the alkali feldspars can be excluded comparing the enthalpies and entropies of several Na–K exchange reactions with those of Na–K geothermometers, as discussed in Sect. 5.3.3.

R. Cioni and L. Marini, *A Thermodynamic Approach to Water Geothermometry*, Springer Geochemistry, https://doi.org/10.1007/978-3-030-54318-1_6

6.1 The Log K of the Na–K Exchange Reactions Between Hydrothermal Alkali Feldspars

Since hydrothermal Na- and K-feldspars are pure or relatively pure minerals (see Sect. 4.2.2), their activities can be considered to be close to unity and the equilibrium constant of reaction (6.1) can be simplified as follows:

$$K = \frac{a_{K-feldspar} \cdot a_{Na^+}}{a_{Na-feldspar} \cdot a_{K^+}} \cong \frac{a_{Na^+}}{a_{K^+}}. \tag{6.2}$$

Equation (6.2) indicates that the Na^+/K^+ activity ratio of reservoir liquids is expected to be a simple temperature function, thus supporting the use of the Na^+/K^+ activity ratio or, to a first approximation, of the Na/K concentration ratio for geothermometry. However, the different structural state of the alkali feldspars and Al-Si order-disorder on their tetrahedral sites complicate this simple picture, making unlikely the existence of a unique Na–K geothermometer applicable everywhere, as underscored by Bird and Norton (1981) and already noted in Sect. 5.3.4.

Although the reasons for choosing the thermodynamic data of the alkali feldspars given by Helgeson et al. (1978) to derive the activity-based Na–K theoretical indicators of interest were thoroughly explained in Sect. 4.2.3, it is interesting to make a brief digression to see how the choice of thermodynamic properties of the alkali feldspars other than those of Helgeson et al. (1978) impacts the temperature dependence of the Na/K log activity ratio.

First, the thermodynamic equilibrium constant of the exchange reactions involving the four endmember alkali feldspars, that is the log K values of the exchange reactions between low-albite and maximum-microcline, low-albite and high-sanidine, high-albite and maximum-microcline, high-albite and high-sanidine were calculated by means of SUPCRT92 considering the thermodynamic data of Helgeson et al. (1978). Results of these SUPCRT92 calculations are shown in Fig. 6.1. Extrapolation of the lines for these four exchange reactions above 350 °C shows that the low-albite/maximum-microcline line intersects the low-albite/high-sanidine line at 500 °C and the high-albite/maximum-microcline line crosses the high-albite/high-sanidine line at the same temperature, which is the microcline-sanidine transition temperature consistent with the thermodynamic data of Helgeson et al. (1978) for these two K-feldspars, as discussed in Sect. 4.2.4. In other terms, the equality of the log K of the low-albite/high-sanidine and low-albite/maximum-microcline exchange reactions at 500 °C and the equality of the log K of the high-albite/high-sanidine and high-albite/maximum-microcline exchange reactions at the same temperature are not fortuitous coincidences, but the consequences of the condition $\Delta G^{\circ}_{f,Sa} = \Delta G^{\circ}_{f,Mc}$ at 500 °C.

Second, the thermodynamic equilibrium constants of the four exchange reactions involving the four endmember alkali feldspars were calculated using SUPCRT92 taking into account the thermodynamic properties of alkali feldspars of Holland and Powell (1998). Results are displayed in Fig. 6.2. Comparison of Figs. 6.1 and 6.2

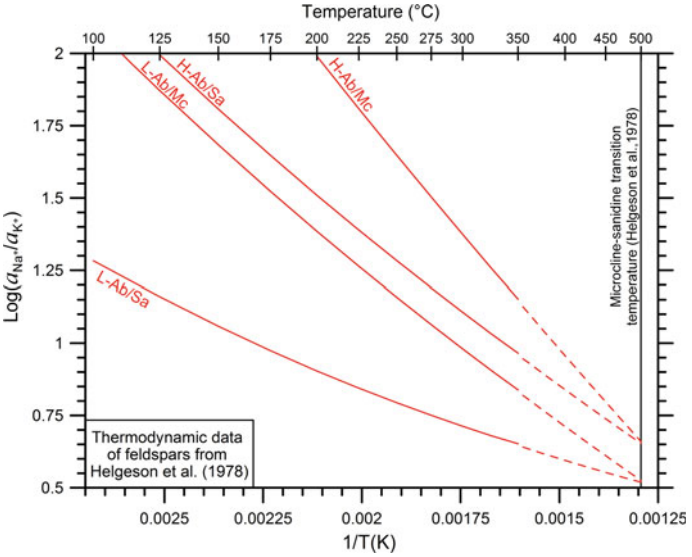

Fig. 6.1 Na/K log activity ratios fixed by low-albite/maximum-microcline (L-Ab/Mc), low-albite/high-sanidine (L-Ab/Sa), high-albite/maximum-microcline (H-Ab/Mc), and high-albite/high-sanidine (H-Ab/Sa) coexistence (red lines, solid below 350 °C, dashed above 350 °C), all computed considering the thermodynamic data of alkali feldspars of Helgeson et al. (1978)

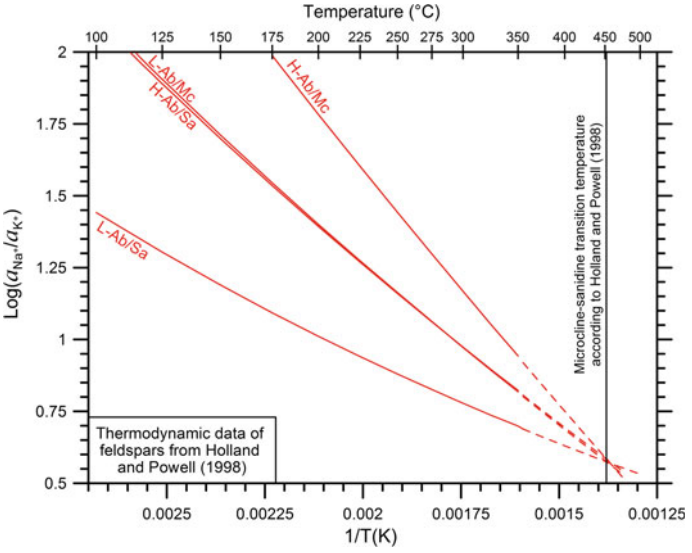

Fig. 6.2 Na/K log activity ratios fixed by low-albite/maximum-microcline (L-Ab/Mc), low-albite/high-sanidine (L-Ab/Sa), high-albite/maximum-microcline (H-Ab/Mc), and high-albite/high-sanidine (H-Ab/Sa) coexistence (red lines, solid below 350 °C, dashed above 350 °C), all computed considering the thermodynamic data of alkali feldspars of Holland and Powell (1998)

shows that the low-albite/maximum-microcline line in Fig. 6.2 is practically superimposed onto the same line in Fig. 6.1, whereas the low-albite/high-sanidine line in Fig. 6.2 is moderately shifted upwards with respect to the same line in Fig. 6.1. These small differences in the position of the low-albite/maximum-microcline and low-albite/high-sanidine lines in Figs. 6.1 and 6.2 reflect the relatively limited difference, ~50 °C, between the sanidine/microcline transition temperature consistent with the thermodynamic data adopted by Holland and Powell (1998) for the two K-feldspars, 452 °C, and the sanidine/microcline transition temperature of Helgeson et al. (1978), 500 °C. To be noted also that the high-albite/maximum-microcline and high-albite/high-sanidine lines in Fig. 6.2 are somewhat shifted downwards compared to the corresponding lines in Fig. 6.1, but also these two lines intersect at the sanidine/microcline transition temperature of 452 °C.

Third, the log K values of the exchange reactions involving the four endmember alkali feldspars were computed by means of SUPCRT92 considering the thermodynamic data of alkali feldspars of Arnórsson and Stefánsson (1999). The outcomes of these calculations are presented in Fig. 6.3.

In Fig. 6.3, the low-albite/high-sanidine line intersects the steeper low-albite/maximum-microcline line at 210 °C and the high-albite/high-sanidine line crosses the steeper high-albite/maximum-microcline line at the same temperature, which is the sanidine/microcline transition temperature consistent with the thermodynamic data of Arnórsson and Stefánsson (1999) for the two K-feldspars, as shown in Sect. 4.2.4.

Summing up, the comparison of Figs. 6.1, 6.2, and 6.3 shows that the sanidine/microcline transition temperature constrains the temperature—log K relations

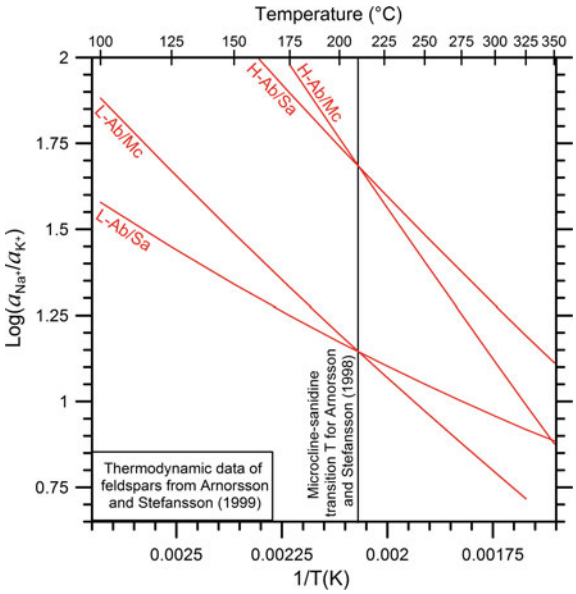

Fig. 6.3 Na/K log activity ratios fixed by low-albite/maximum microcline (L-Ab/Mc), low-albite/high-sanidine (L-Ab/Sa), high-albite/maximum-microcline (H-Ab/Mc), and high-albite/high-sanidine (H-Ab/Sa) coexistence (red solid lines), all computed considering the thermodynamic data of alkali feldspars of Arnórsson and Stefánsson (1999)

of the exchange reactions between alkali feldspars. Therefore, it is of utmost importance to rely on thermodynamic data of alkali feldspars which are consistent with the correct sanidine/microcline transition temperature, like those of Helgeson et al. (1978). Another good reason for choosing the thermodynamic data of Helgeson et al. (1978), not only for the alkali feldspars but also for all the other solid phases, is the high level of internal consistency of this thermodynamic database as already recalled in Sect. 2.2. Moreover, the shifts in the thermodynamic data of the Al-bearing solid phases with respect to other datasets do not affect the thermodynamic properties of the reactions of interest to us, owing to Al conservation in the solid phases.

Resuming the main discussion, it must be underscored that the hydrothermal feldspars participating to reaction (6.1) are most likely triclinic, fully-ordered low-albite and variably-ordered adularia, from fully ordered microcline to completely disordered sanidine, with either triclinic or monoclinic symmetry, as discussed in Sects. 4.2.3 and 5.3.3. Accepting this hypothesis, the Na/K activity ratio is expected to be a function of both temperature and the ordering parameter of adularia, Z, which is equal to 1 for maximum-microcline and assumes the value of 0 for high-sanidine. Therefore, the logarithm of the thermodynamic equilibrium constant of reaction (6.1), involving low-albite and adularia with variable ordering parameter Z, was computed using SUPCRT92 considering the thermodynamic data of alkali feldspars of Helgeson et al. (1978) for temperatures varying from 0 to 350 °C at steps of 25 °C and for Z values ranging from 0 to 1 at steps of 0.1 Z units. Results are reported in Table 6.1.

The computed log K values are nearly equal to the Na^+/K^+ activity ratio and are reproduced with acceptable approximations by the following two equations (T in °C):

$$\begin{aligned} Z = &\left(2.1911 \cdot 10^{-7} \cdot T^3 - 8.9451 \cdot 10^{-5} \cdot T^2 + 2.0023 \cdot 10^{-2} \cdot T - 0.11043\right) \\ &\cdot \log(a_{Na^+}/a_{K^+}) - 1.1269 \cdot 10^{-7} \cdot T^3 + 4.2393 \cdot 10^{-5} \cdot T^2 \\ &- 7.8201 \cdot 10^{-3} \cdot T - 1.1045 \end{aligned} \tag{6.3}$$

$$\begin{aligned} &1000/(T + 273.15) = \\ &\left(-0.919194 \cdot Z^4 + 2.759529 \cdot Z^3 - 3.361149 \cdot Z^2 + 2.209325 \cdot Z - 0.791765\right) \\ &\cdot \left[\log(a_{Na^+}/a_{K^+})\right]^2 + \left(1.5035 \cdot Z^4 - 4.717177 \cdot Z^3 + 6.31701 \cdot Z^2 - 5.16263 \cdot Z + 3.215553\right) \\ &\cdot \log(a_{Na^+}/a_{K^+}) - 0.51088 \cdot Z^4 + 1.632504 \cdot Z^3 - 2.275505 \cdot Z^2 \\ &+ 2.011206 \cdot Z - 0.147528 \end{aligned} \tag{6.4}$$

which are valid from 100 to 350 °C and can be alternatively used depending on what we know and what we want to compute.

Table 6.1 Logarithm of the thermodynamic equilibrium constant of the exchange reaction (6.1) involving low-albite and adularia with ordering parameter Z varying from 1 to 0 at steps of 0.1 units, as a function of temperature and the Z ordering parameter of adularia

T(°C)	Z = 1	Z = 0.9	Z = 0.8	Z = 0.7	Z = 0.6	Z = 0.5	Z = 0.4	Z = 0.3	Z = 0.2	Z = 0.1	Z = 0
0.01	3.4941	3.3564	3.2188	3.0811	2.9434	2.8057	2.668	2.5303	2.3926	2.2549	2.1172
25	3.0398	2.9199	2.7999	2.68	2.5601	2.4402	2.3203	2.2003	2.0804	1.9605	1.8406
50	2.6647	2.5598	2.4549	2.35	2.2451	2.1402	2.0353	1.9304	1.8255	1.7206	1.6157
75	2.3530	2.2609	2.1689	2.0769	1.9849	1.8928	1.8008	1.7088	1.6168	1.5247	1.4327
100	2.0919	2.0110	1.9301	1.8492	1.7683	1.6874	1.6066	1.5257	1.4448	1.3639	1.2830
125	1.8714	1.8003	1.7291	1.6580	1.5869	1.5157	1.4446	1.3735	1.3023	1.2312	1.1600
150	1.6839	1.6213	1.5588	1.4963	1.4337	1.3712	1.3086	1.2461	1.1835	1.1210	1.0584
175	1.5232	1.4683	1.4134	1.3585	1.3036	1.2487	1.1937	1.1388	1.0839	1.0290	0.9741
200	1.3846	1.3365	1.2884	1.2403	1.1923	1.1442	1.0961	1.0480	0.9999	0.9518	0.9038
225	1.2641	1.2221	1.1802	1.1382	1.0963	1.0544	1.0124	0.9705	0.9285	0.8866	0.8446
250	1.1583	1.1219	1.0855	1.0491	1.0127	0.9763	0.9399	0.9035	0.8671	0.8307	0.7943
275	1.0643	1.0329	1.0016	0.9702	0.9389	0.9075	0.8762	0.8449	0.8135	0.7822	0.7508
300	0.9802	0.9533	0.9266	0.8999	0.8731	0.8464	0.8196	0.7929	0.7662	0.7394	0.7127
325	0.9049	0.8823	0.8598	0.8372	0.8147	0.7922	0.7697	0.7471	0.7246	0.7021	0.6796
350	0.8388	0.8200	0.8013	0.7827	0.7640	0.7454	0.7267	0.7081	0.6895	0.6708	0.6522

Z = 1 corresponds to maximum-microcline and Z = 0 corresponds to high-sanidine. P = 1 bar for T < 100 °C; P = P_{sat} for T ≥ 100 °C. Calculations performed using SUPCRT92 considering the thermodynamic data of alkali feldspars of Helgeson et al. (1978)

6.2 The Na^+/K^+ Log Activity Ratio of the Selected Reservoir Liquids

Let us now consider the binary plots in which the Na^+/K^+ log activity ratio is contrasted with the aquifer temperature inverse for the selected reservoir liquids of Iceland (Fig. 6.4a), Northern and Central America (Fig. 6.4b), Japan (Fig. 6.5a), the Philippines (Fig. 6.5b), New Zealand (Fig. 6.6a), and miscellaneous systems (Fig. 6.6b).

The Na^+/K^+ log activity ratios fixed by low-albite/maximum-microcline, low-albite/high-sanidine, high-albite/maximum-microcline, and high-albite/high-sanidine equilibrium coexistence, as well as by equilibrium co-occurrence of low-albite and adularia with ordering parameter Z varying from 0 to 1 at steps of 0.1 units, all computed considering the thermodynamic data of alkali feldspars of Helgeson et al. (1978) are also shown in these diagrams for comparison.

In these binary plots, 950 of the 1013 reservoir liquids (corresponding to 93.8% of the total) are found between the lines of low-albite/maximum microcline and low-albite/high-sanidine equilibrium coexistence, 19 samples only (1.9% of the total) are located above the low-albite/maximum microcline line and 45 samples only (4.4% of the total) are situated below the low-albite/high-sanidine line. Moreover, the 64 samples positioned outside the field of low-albite/adularia equilibrium co-occurrence exhibit small or relatively small deviations.

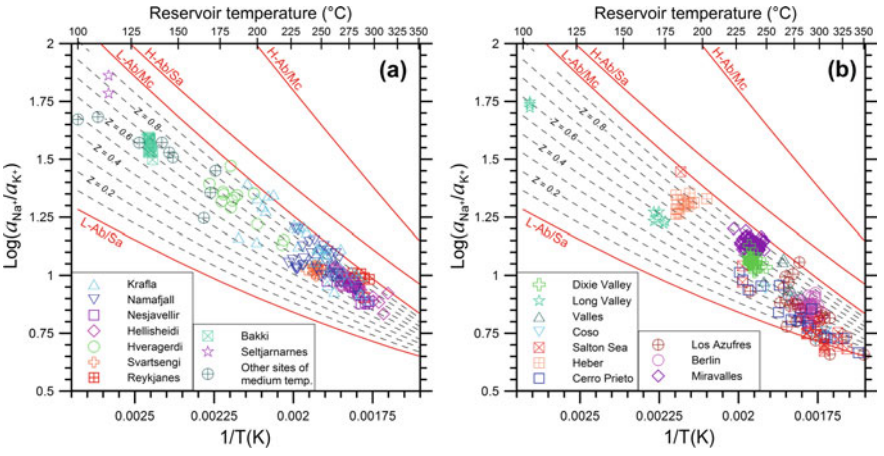

Fig. 6.4 Na^+/K^+ log activity ratios of the selected reservoir liquids of (a) Iceland and (b) North and Central America as a function of aquifer temperature. Also shown are the Na^+/K^+ log activity ratios fixed by low-albite/maximum-microcline (L-Ab/Mc), low-albite/high-sanidine (L-Ab/Sa), high-albite/maximum-microcline (H-Ab/Mc), and high-albite/high-sanidine (H-Ab/Sa) equilibrium coexistence (red solid lines), as well as by equilibrium co-occurrence of low-albite and adularia with ordering parameter Z varying from 0 to 1 at steps of 0.1 units (dashed black lines)

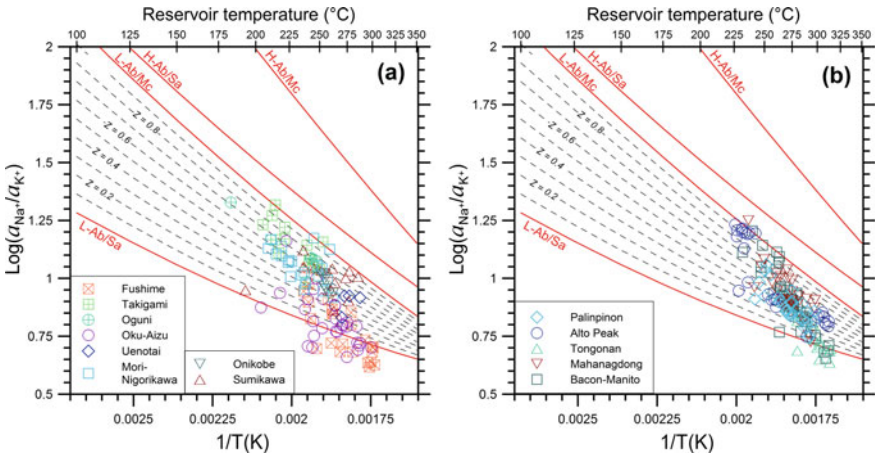

Fig. 6.5 Na^+/K^+ log activity ratios of the selected reservoir liquids of **a** Japan and **b** The Philippines as a function of aquifer temperature. Also shown are the Na^+/K^+ log activity ratios fixed by low-albite/maximum-microcline (L-Ab/Mc), low-albite/high-sanidine (L-Ab/Sa), high-albite/maximum-microcline (H-Ab/Mc), and high-albite/high-sanidine (H-Ab/Sa) equilibrium coexistence (red solid lines), as well as by equilibrium co-occurrence of low-albite and adularia with ordering parameter Z varying from 0 to 1 at steps of 0.1 units (dashed black lines)

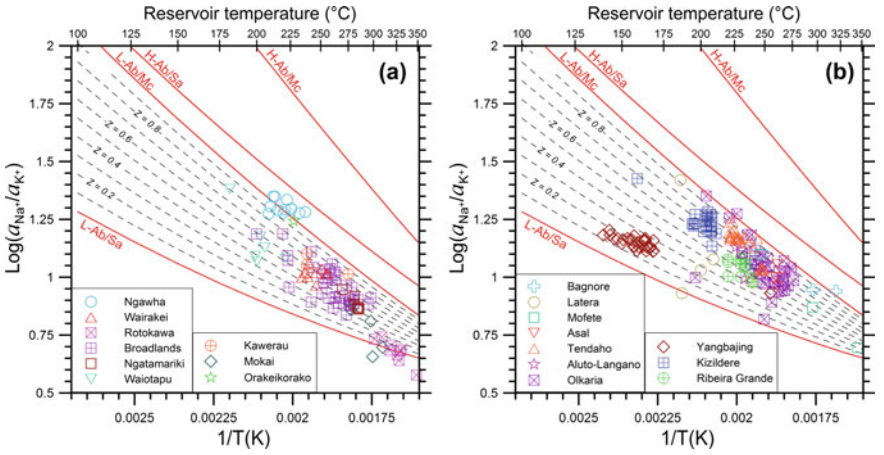

Fig. 6.6 Na^+/K^+ log activity ratios of the selected reservoir liquids of **a** New Zealand and **b** miscellaneous systems as a function of aquifer temperature. Also shown are the Na^+/K^+ log activity ratios fixed by low-albite/maximum-microcline (L-Ab/Mc), low-albite/high-sanidine (L-Ab/Sa), high-albite/maximum-microcline (H-Ab/Mc), and high-albite/high-sanidine (H-Ab/Sa) equilibrium coexistence (red solid lines), as well as by equilibrium co-occurrence of low-albite and adularia with ordering parameter Z varying from 0 to 1 at steps of 0.1 units (dashed black lines)

Of the 19 samples with Na^+/K^+ log activity ratios weakly higher than those fixed by low-albite/maximum microcline equilibrium coexistence, 2 are from Krafla (Fig. 6.4a), 1 is from Los Azufres (Fig. 6.4b), 2 are from Takigami, 1 is from Mori-Nigorikawa (Fig. 6.5a), 1 each are from Mahanagdong, Bacon Manito, and Alto Peak (Fig. 6.5b), 8 are from Ngawha (Fig. 6.6a), 1 is from Bagnore, and 1 is from Olkaria (Fig. 6.6b). These small deviations are attributable to distinct reasons, including the undersaturation with completely ordered adularia[1], overestimation of aquifer temperature, underestimation of K^+ ion activity, and overestimation of Na^+ ion activity. The 12 reservoir liquids of Ngawha and the 2 reservoir liquids of Bagnore are unique due to the high concentrations of dissolved B (760–1026 mg/kg at Ngawha; 299 and 459 mg/kg at Bagnore) and NH_4 (69–293 mg/kg at Ngawha, 438 and 669 mg/kg at Bagnore). Since B^{3+} can be hosted in the T-sites of alkali feldspars substituting for Al^{3+} ion and NH_4^+ ion can occupy the M-sites of alkali feldspars replacing for Na^+ and K^+ ions (see Sect. 4.2.1), the hydrothermal alkali feldspars occurring in the Ngawha and Bagnore geothermal reservoirs might be different from pure albite and adularia. If so, the activity of albite and adularia would be different from unity, and should be properly considered in Eq. (6.2). Unfortunately, we were not able to find chemical analyses of the hydrothermal alkali feldspars present in the Ngawha and Bagnore geothermal aquifers to further investigate this matter.

Of the 45 samples with Na^+/K^+ log activity ratios slightly lower than those fixed by low-albite/high-sanidine equilibrium co-occurrence, 5 are from Salton Sea, 1 is from Los Azufres (Fig. 6.4b), 12 each are from Fushime and Oku-Aizu (Fig. 6.5a), 5 are from Tongonan, 4 are from Bacon-Manito (Fig. 6.5b), 4 are from Rotokawa and 2 are from Mokai (Fig. 6.6a). These limited deviations might be due to different causes, such as supersaturation with fully disordered adularia, underestimation of aquifer temperature, overestimation of K^+ ion activity, and underestimation of Na^+ ion activity. Furthermore, given the high temperatures and high salinities of some of these aqueous solutions, firstly those of Salton Sea and secondly those of Fushime and Oku-Aizu, the activities of Na^+ and K^+ ions might be affected by uncertainties in speciation calculations.

Most reservoir liquids of Northern-Central America (Fig. 6.4b), Japan (Fig. 6.5a), The Philippines (Fig. 6.5b), and New Zealand (Fig. 6.6a)are characterized by a general decrease in Z with increasing temperature in spite of the considerable scatter of sample points. In contrast, most reservoir liquids of Iceland have Z values ranging from 0.5 to 1 irrespective of temperature (Fig. 6.4a).

All in all, the spread of sample points in the binary plots of Figs. 6.4, 6.5 and 6.6 is in accordance with the expectations based on the characteristics of authigenic feldspars occurring in sedimentary rocks and to some extent in low-temperature hydrothermal veins as well as of K-feldspars and albites synthesized in hydroxide gels (Sect. 4.2.3). This suggests that the Na^+/K^+ log activity ratio of reservoir liquids is usually controlled by equilibrium coexistence of fully ordered low-albite and adularia with ordering parameter Z varying from 0 to 1. This inference is supported by a large

[1] Saturation with low-albite was assumed in speciation calculation to fix Al concentration.

number of data above ~200 °C, but is probably valid also in the temperature range 100–200 °C, in spite of the lower number of available data.

6.3 The Ordering Parameter Z of Hydrothermal Adularia in Hypothetical Equilibrium with the Selected Reservoir Liquids

The ordering parameter Z of hydrothermal adularia in hypothetical equilibrium with each reservoir liquid of interest was computed by inserting its Na^+/K^+ log activity ratio and reservoir temperature into Eq. (6.3). Considering together the 1013 selected reservoir liquids, Z has a mean of 0.559, a median of 0.612, and a standard deviation of 0.261. These statistical parameters were calculated forcing to 1 the 19 values of Z higher than 1 and forcing to 0 the 45 values of Z lower than 0. The main statistical parameters of Z for the selected reservoir liquids, divided according to the geothermal field of provenance, are listed in Table 6.2, whereas their mean and median values of Z are contrasted in the binary diagram of Fig. 6.7, in which the error bars correspond to ± 1 standard deviation.

Most geothermal systems have mean value of the ordering parameter Z of hydrothermal adularia in the range 0.347–0.808. The hydrothermal adularia of Bagnore and Ngawha has higher mean Z values, 0.908 and 0.977, respectively. These high means are expected on the basis of the unusual fluid chemistry of these two sites (see above). In contrast, the hydrothermal adularia of Cerro Prieto, Yangbajing, Mokai, Salton Sea, Fushime, Oku-aizu, Tongonan, and Rotokawa has lower average Z values, in the interval 0.047–0.239. The low Z values of hydrothermal adularia in hypothetical equilibrium with the Salton Sea reservoir liquids agree with previous findings of Bird and Helgeson (1981) who recognized that these aqueous solutions are close to equilibrium with an hydrothermal assemblage including high-sanidine, which has $Z = 0$.

For the Na–K geothermometers of Fournier (1979), Arnórsson et al. (1983), Giggenbach (1988), and Arnórsson (2000), which are probably those most widely used, we have computed the ordering parameter Z of hydrothermal adularia as a function of temperature by inserting the Na/K total molality ratio and the corresponding temperature into Eq. (6.3), assuming that the Na/K total molality ratio is equal to the Na^+/K^+ activity ratio. The calculated ordering parameter Z of adularia varies as follows, as shown by the diagram of Fig. 6.8: (i) 0.90 at 100–150 °C, 0.87 at 200 °C, 0.77 at 250 °C, 0.59 at 300 °C, and 0.26 at 350 °C for the function of Fournier (1979); (ii) 0.56 at 100 °C, 0.61 at 150 °C, 0.64 at 200 °C, 0.62 or 0.68 at 250 °C, 0.45 at 300 °C, and 0.00 at 348 °C for the two geothermometers of Arnórsson et al. (1983); (iii) 0.95 at 250 °C, 0.72 at 300 °C, and 0.32 at 350 °C for the geothermometer of Giggenbach (1988); (iv) 0.79 at 100 °C, 0.75 at 150 °C, 0.70 at 200 °C, 0.62 at 250 °C, 0.49 at 300 °C, and 0.24 at 350 °C for the theoretical function of Arnórsson (2000).

Table 6.2 Main statistical parameters for the ordering parameter Z of hydrothermal adularia in hypothetical equilibrium with the reservoir liquids of interest divided according to the field of provenance

Field	Country	N	Minimum	Maximum	Median	Mean	Std.Dev.
Hellisheidi	Iceland	27	0.539	0.949	0.698	0.699	0.080
Hveragerdi	Iceland	13	0.623	0.977	0.702	0.728	0.106
Krafla	Iceland	36	0.437	1.000	0.846	0.795	0.159
Namafjall	Iceland	37	0.460	0.958	0.686	0.704	0.148
Nesjavellir	Iceland	15	0.497	0.754	0.642	0.637	0.080
Reykjanes	Iceland	13	0.621	0.952	0.770	0.779	0.118
Svartsengi	Iceland	12	0.522	0.656	0.593	0.590	0.049
Iceland, medium T	Iceland	29	0.416	0.865	0.668	0.658	0.089
Dixie Valley	USA	35	0.525	0.776	0.627	0.627	0.048
Long Valley	USA	10	0.415	0.603	0.483	0.502	0.065
Valles	USA	7	0.478	0.920	0.580	0.648	0.172
Coso	USA	5	0.006	0.683	0.397	0.347	0.253
Salton Sea	USA	23	0.000	0.962	0.082	0.161	0.222
Heber	USA	16	0.585	0.916	0.716	0.717	0.090
Cerro Prieto	Mexico	19	0.036	0.539	0.193	0.239	0.137
Los Azufres	Mexico	26	0.000	1.000	0.365	0.370	0.242
Berlin	El Salvador	55	0.195	0.749	0.443	0.441	0.117
Miravalles	Costa Rica	105	0.673	0.968	0.801	0.808	0.055
Mori Nigorikawa	Japan	21	0.336	1.000	0.549	0.578	0.169
Sumikawa	Japan	14	0.052	0.928	0.657	0.623	0.240
Uenotai	Japan	4	0.221	0.639	0.550	0.490	0.185
Onikobe	Japan	7	0.438	0.654	0.506	0.540	0.083
Oku-aizu	Japan	31	0.000	0.735	0.074	0.138	0.184
Oguni	Japan	6	0.640	0.743	0.730	0.717	0.039
Takigami	Japan	13	0.421	1.000	0.728	0.749	0.166
Fushime	Japan	25	0.000	0.602	0.037	0.146	0.181
Palinpinon	The Philippines	29	0.065	0.745	0.351	0.378	0.164
Alto Peak	The Philippines	27	0.067	1.000	0.497	0.604	0.278
Tongonan	The Philippines	11	0.000	0.295	0.011	0.064	0.105
Mahanagdong	The Philippines	28	0.006	1.000	0.569	0.554	0.216
Bacon-Manito	The Philippines	51	0.000	1.000	0.434	0.444	0.252
Ngawha	New Zealand	12	0.852	1.000	1.000	0.977	0.045
Kawerau	New Zealand	4	0.515	0.838	0.669	0.673	0.142

(continued)

Table 6.2 (continued)

Field	Country	N	Minimum	Maximum	Median	Mean	Std.Dev.
Waiotapu	New Zealand	6	0.340	0.805	0.521	0.525	0.166
Ngatamariki	New Zealand	7	0.432	0.586	0.458	0.488	0.066
Broadlands + Orakeikorako	New Zealand	42	0.217	0.978	0.557	0.553	0.169
Mokai	New Zealand	4	0.000	0.366	0.172	0.177	0.205
Wairakei	New Zealand	9	0.434	0.675	0.585	0.563	0.098
Rotokawa	New Zealand	9	0.000	0.165	0.031	0.047	0.057
Bagnore	Italy	2	0.817	1.000	0.908	0.908	0.130
Latera	Italy	5	0.000	0.923	0.419	0.406	0.337
Mofete	Italy	3	0.197	0.807	0.541	0.515	0.306
Asal	Djibouti	4	0.545	0.826	0.651	0.668	0.117
Tendaho	Ethiopia	36	0.609	0.950	0.792	0.771	0.087
Aluto-Langano	Ethiopia	3	0.408	0.837	0.686	0.644	0.217
Olkaria	Kenya	42	0.064	1.000	0.675	0.673	0.199
Yangbajing	China	32	0.127	0.415	0.204	0.214	0.067
Kizildere	Turkey	28	0.544	0.838	0.702	0.714	0.078
Ribeira Grande	Azores, Portugal	15	0.343	0.638	0.532	0.517	0.084

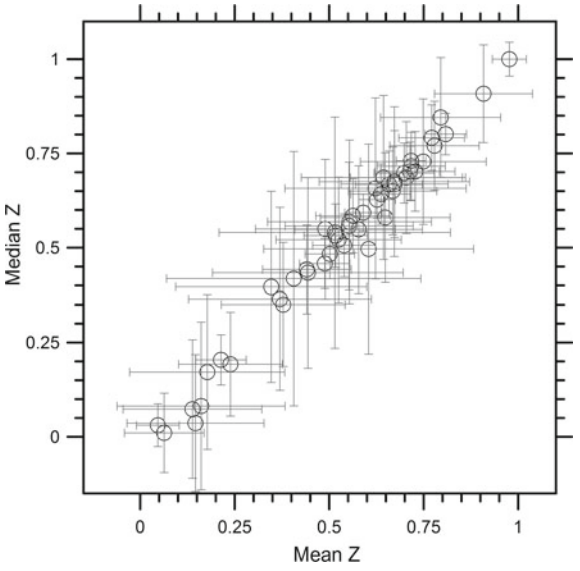

Fig. 6.7 Correlation plot between the mean and median values of the ordering parameter Z of hydrothermal adularia in hypothetical equilibrium with the considered reservoir liquids divided according to the field of provenance. The error bars correspond to ±1 standard deviation

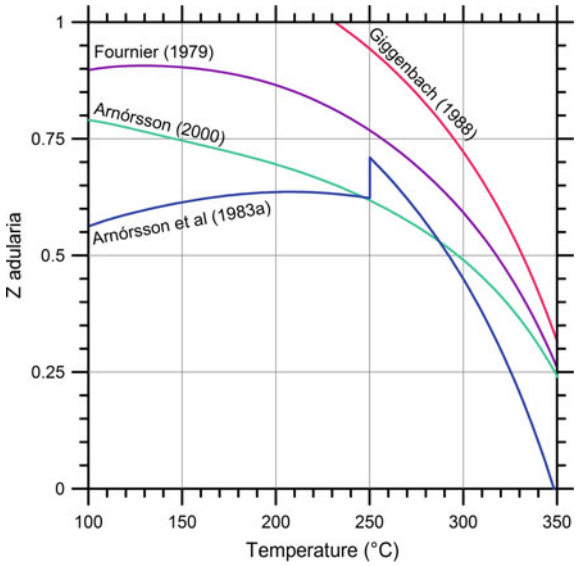

Fig. 6.8 Ordering parameter Z of hydrothermal adularia involved in the Na–K geothermometers of Fournier (1979), Arnórsson et al. (1983), Giggenbach (1988), and Arnórsson (2000), as a function of temperature

In spite of the considerable differences among these four Na–K geothermometers, they exhibit a common decrease in Z with increasing temperature, thus mimicking the general trend described by most data in the correlation diagrams of Figs. 6.4, 6.5 and 6.6.

6.4 The Theoretical Activity-Based Na–K Geothermometers Involving the Ordering Parameter of Adularia

In Figs. 6.4, 6.5 and 6.6 most considered reservoir liquids, presumably representative of mineral-solution equilibrium, are found above the line fixed by equilibrium coexistence of low-albite and high-sanidine and below the line constrained by equilibrium co-occurrence of low-albite and maximum-microcline. Consequently, the two corresponding geothermometric functions can be used to calculate the minimum and maximum Na–K equilibrium temperatures, respectively. These two theoretical activity-based Na–K geothermometers are described by the following two polynomial equations[2], in which $\beta = \log(a_{Na^+}/a_{K^+})$:

[2]In Figs. 6.4, 6.5 and 6.6, pronounced deviations from linearity can be observed for all the functions outlining the temperature dependence of the Na^+/K^+ log activity ratio, not only those fixed by low-albite/maximum-microcline and low-albite/high-sanidine equilibrium coexistence, but also those constrained by equilibrium co-occurrence of low-albite and adularia with ordering parameter

$$T_{Na-K(Z=0)}(°C) = 300.04 \cdot \beta^4 - 1736.7 \cdot \beta^3 + 3813.9 \cdot \beta^2 - 3923.2 \cdot \beta + 1711.6 \tag{6.5}$$

$$T_{Na-K(Z=1)}(°C) = 12.909 \cdot \beta^4 - 126.80 \cdot \beta^3 + 488.60 \cdot \beta^2 - 955.91 \cdot \beta + 875.63. \tag{6.6}$$

Equations (6.4) and (6.5) are applicable in the range 25–350 °C and the uncertainty in the computed temperature varies from 0.1 to 1 °C. Nevertheless, use of Eqs. (6.5) and (6.6) is not advisable below 100 °C, and sometimes even below 150 °C, owing to the marked decrease in the rate of the dissolution/precipitation reactions of alkali feldspars with decreasing temperature (e.g., Palandri and Kharaka 2004, Marini 2006, Bandstra et al. 2008 and references therein). Regardless of these considerations on reaction kinetics, the usefulness of Eqs. (6.4) and (6.5) is very limited because the Na–K-temperatures computed for Z = 0 and Z = 1 differ by 125 ± 3 °C on average, in the range 100–350 °C.

Therefore, it would be desirable to adopt a different approach to Na–K geothermometry, such as that consisting in the following two steps:

1. Calculation of the ordering parameter of adularia presumably in equilibrium with the aqueous solution of interest, based on either the logarithm of the total concentration of dissolved components (e.g., B, SiO_2, Na, K, Mg, Ca, SO_4, Cl, ΣCO_2, and ΣH_2S) or the logarithm of the activity of the related ionic or neutral species (e.g., $H_3BO_{3,aq}$, $SiO_{2,aq}$, Na^+, K^+, Mg^{2+}, Ca^{2+}, $SO_4{}^{2-}$, Cl^-, $HCO_3{}^-$, and HS^-), assuming that the degree of ordering of adularia is somehow related to water chemistry, as suggested by the experimental synthesis of alkali feldspars in hydroxide gels (see Sect. 4.2.3).
2. Use of the Z value obtained from water chemistry and the Na^+/K^+ activity ratio to compute the Na–K temperature of the aqueous solution of interest by means of Eq. (6.4).

Several attempts were done to find a suitable relation for predicting Z from water chemistry. Use of Factor Analysis (FA) followed by Multiple Regression Analysis (MRA) was explored to avoid multicollinearity issues, but the obtained relations resulted to be poor predictors due to the low R-squared values.

Therefore, MRA only was utilized, in spite of the high inter-associations among the independent variables. Different MRA runs were performed considering the selected reservoir liquids either altogether or in separate groups, but it turned out that Z is chiefly controlled by Na, K, and SiO_2 in all these attempts. This is a disappointing result being affected by a circular argument as explained, in more detail, referring to the following equation:

$$Z = 1.97264 - 2.24782 \cdot \log a_{K^+} + 2.19929 \cdot \log a_{Na^+} + 1.77758 \cdot \log a_{SiO_{2(aq)}}, \tag{6.7}$$

Z varying from 0 to 1 at steps of 0.1 units. Consequently, the use of polynomial equations of temperature, instead of linear functions of the absolute temperature inverse, is advisable (if not mandatory) for obtaining the desired Na–K activity-based theoretical geothermometers.

which was obtained considering the 1013 samples altogether in MRA. Equation (6.7) has standard errors of 0.057203 on the intercept, 0.033916 on the coefficient of $\log a_{K^+}$, 0.036593 on the coefficient of $\log a_{Na^+}$, and 0.038055 on the coefficient of $\log a_{SiO_{2(aq)}}$. Equation (6.7) has multiple R of 0.9138, multiple R-squared of 0.8351, and adjusted multiple R-squared of 0.8346. The standard error on the predicted Z values is 0.114, which is a relatively high value. For instance, for $\log(a_{Na^+}/a_{K^+}) = 1$, the corresponding error on the computed Na–K temperature is of 11–18 °C.

However, it must be noted that the coefficients of $\log a_{Na^+}$ and $\log a_{K^+}$ are positive and negative, respectively, but have almost the same absolute value, whereas $\log a_{SiO_{2(aq)}}$ is a proxy of temperature. Thus, Eq. (6.7) expresses the dependence of Z on $\log(a_{Na^+}/a_{K^+})$ and temperature and, therefore, is affected by a circular argument because Z was previously computed by inserting $\log(a_{Na^+}/a_{K^+})$ and temperature into Eq. (6.3). In short words, Eq. (6.7) and similar relations are meaningless.

6.5 Final Considerations on the Use of the Na/K-Activity Ratio

To conclude this chapter, it is worth repeating that a single universally-working Na–K geothermometer does not exist, regardless of whether it is calibrated empirically or it is based on the solid pillars of thermodynamics. This is due to the different degree of Al–Si order-disorder on the tetrahedral sites of alkali feldspars, as already pointed out by Bird and Norton (1981).

For this reason, Na–K geothermometry must necessarily imply the ordering parameter of adularia, Z. The two limiting Na–K geothermometers, involving low-albite and either high-sanidine or maximum-microcline, as proxies of completely disordered adularia (with $Z = 0$) and totally ordered adularia (with $Z = 1$), respectively, give equilibrium temperatures differing by 125 ± 3 °C on average, in the range 100–350 °C, and have little usefulness. The attempts that we carried out to predict Z on the basis of water chemistry were unsuccessful, but it is possible that the available data are inadequate and that this matter might be clarified by further researches.

All in all, for the moment, it is probably advisable to use the Na/K log activity ratio to estimate the ordering parameter Z of the hydrothermal adularia in hypothetical equilibrium with the aqueous solution of interest and to use this information in other geothermometric functions that are presented and discussed in the following chapters.

References

Arnórsson S (2000) The quartz and Na/K geothermometers. I. New thermodynamic calibration. In: Proceedings of the world geothermal congress 2000. Kyushu-Tohoku, Japan, pp 929–934

Arnórsson S, Stefánsson A (1999) Assessment of feldspar solubility constants in water in the range of 0–350 °C at vapor saturation pressures. Am J Sci 299:173–209

Arnórsson S, Gunnlaugsson E, Svavarsson H (1983) The chemistry of geothermal waters in Iceland. III. Chemical geothermometry in geothermal investigations. Geochim Cosmochim Ac 47:567–577

Bandstra JZ, Buss HL, Campen RK, Liermann LJ, Moore J, Hausrath EM, Navarre-Sitchler A, Jang J-H, Brantley SL (2008) Appendix: Compilation of mineral dissolution rates. In: Brantley SL, Kubicki JD, White AF (eds) Kinetics of water-rock interaction, Springer, New York, pp 737–823

Bird DK, Norton DL (1981) Theoretical prediction of phase relations among aqueous solutions and minerals: Salton Sea geothermal system. Geochim Cosmochim Ac 45:1479–1494

Ellis AJ (1970) Quantitative interpretation of chemical characteristics of hydrothermal systems. Geothermics 2:516–528

Fournier RO (1979) A revised equation for the Na/K geothermometer. Geotherm Res Counc Trans 5:1–16

Giggenbach WF (1988) Geothermal solute equilibria. Derivation of Na–K–Mg–Ca geoindicators. Geochim Cosmochim Ac 52:2749–2765

Helgeson HC, Delany JM, Nesbitt HW, Bird DK (1978) Summary and critique of the thermodynamic properties of rock-forming minerals. Am J Sci 278A:229

Holland TJB, Powell R (1998) An internally consistent thermodynamic data set for phases of petrological interest. J Metamorph Geol 16:309–343

Marini L (2006) Geological sequestration of carbon dioxide: Thermodynamics, kinetics, and reaction path modeling. Developments in geochemistry, 11. Elsevier, Amsterdam, p 453

Michard G (1990) Behaviour of major elements and some trace elements (Li, Rb, Cs, Sr, Fe, Mn, W, F) in deep hot waters from granitic areas. Chem Geol 89:117–134

Palandri JL, Kharaka YK (2004) A compilation of rate parameters of water-mineral interaction kinetics for application to geochemical modeling. US Geological Survey, Open File Report 2004–1068

White DE (1965) Saline waters of sedimentary rocks. In Fluids in Subsurface Environments. Symp Amer Assoc Petroleum Geologists 342–366